

Vanadium Oxide Incorporated into Mesoporous Titania with a BET Surface Area above 1000 m²·g⁻¹: Preparation, Spectroscopic Characterization, and Catalytic Oxidation

Hideaki Yoshitake*[†] and Takashi Tatsumi[‡]

Graduate School of Environment and Information Sciences, and Division of Material Sciences and Chemical Engineering, Graduate School of Engineering, Yokohama National University, 79-7 Tokiwadai, Hodogaya-ku, Yokohama 240-8501, Japan

Received November 5, 2002. Revised Manuscript Received February 12, 2003

To reveal the potential properties of mesoporous titania with a BET surface area of more than 1000 m²·g⁻¹, we incorporated vanadium into mesoporous titania by co-condensation (direct incorporation, V-meso TiO₂) and by postsynthesis impregnation (impregnation, V/meso TiO₂). The mesostructure remained until the loading reached 5 wt % as V metal for V-meso TiO₂. The catalysts were characterized by transmission XANES and room-temperature ESR spectroscopies. The pre-edge absorption in V K edge spectra of V-meso TiO₂ demonstrated that the valence of V is 4+ under atmospheric conditions (i.e., exposed to air and at room temperature). Ti K edge XANES showed that 5-fold coordinated Ti, which originally comprised 37% of the total titanium in the mesoporous titania, was substituted by V. In contrast, V in V/meso TiO₂ was assigned to a valence of 5+. In ESR spectra, both of these catalysts showed strong *hfs* multiples characteristic of isolated vanadyl species in either square pyramidal or distorted octahedral coordination. The pattern of V⁴⁺ in V-meso TiO₂ did not change by evacuation at 473 K, implying an extremely stabilized tetravalent state in mesoporous titania. Both V-meso TiO₂ and V/meso TiO₂ were highly active in a propene oxidation reaction. The oxidation rates per unit V were much enhanced from the activity of highly dispersed V/JRC-TIO-4 (conventional nonporous titania support).

Introduction

Transition metal substituted M41S molecular sieves are of current interest as catalysts for the oxidation of a variety of compounds.^{1,2} These molecular sieve silicas possess uniform mesopore channels, which vary from 2 to 10 nm, and a large surface area usually more than 800 m²·g⁻¹. These are advantageous characteristics for a catalytic support because the mesopores can accommodate larger molecules than the micropore channels and a high dispersion of catalytically active species is easily achieved due to the large surface area. Because supported vanadia catalysts are widely used for the partial oxidation of organic compounds such as methanol,³ aromatic compounds,^{4–6} and olefins,^{7,8} the am-

oxidation of aromatic hydrocarbons⁹ and the selective catalytic reduction of NO_x,^{10,11} a number of recent studies have been devoted to the synthesis and characterization of V-substituted mesoporous silicas such as MCM-41,^{12–16} MCM-48,^{12,17–20} and SBA-15.²¹

Although intensive research has been carried out on vanadium-substituted silicas, mesoporous transition

* To whom correspondence should be addressed. Fax: +81-45-339-4378. Phone: +81-45-339-4359. E-mail: yos@ynu.ac.jp.

[†] Graduate School of Environment and Information Sciences.

[‡] Division of Material Sciences and Chemical Engineering, Graduate School of Engineering.

(1) Tuel, A. *Microporous Mesoporous Mater.* **1999**, *27*, 151, and references therein.

(2) Corma, A. *Top. Catal.* **1997**, *4*, 249, and references therein.

(3) Wong, G. S.; Kragten, D. D.; Vohs, J. M. *J. Phys. Chem. B* **2001**, *105*, 1366.

(4) Bulushev, D. A.; Kiwi-Minsker, L.; Zaikovskii, V. I.; Renken, A. *J. Catal.* **2000**, *193*, 145.

(5) Gąsior, M.; Gąsior, I.; Grzybowska, B. *Appl. Catal.* **1984**, *10*, 87.

(6) Lars, S.; Andersen, T.; Järås, S. *J. Catal.* **1980**, *64*, 51.

(7) Fierro, J. L. G.; Arrua, L. A.; Lopez Nieto, J. M.; Kremic, G. *Appl. Catal.* **1988**, *37*, 323.

(8) Bond, G. C.; Sarkany, A. J.; Parfitt, G. D. *J. Catal.* **1979**, *57*, 476.

(9) Roussel, H.; Mehlomakulu, B.; Belhadj, F.; van Steen, E.; Millet, J. M. M. *J. Catal.* **2002**, *205*, 97.

(10) Topsøe, N.-Y.; Topsøe, H.; Dumesic, J. A. *J. Catal.* **1995**, *151*, 226.

(11) Georgiadou, I.; Papadopoulou, C.; Matralis, H. K.; Voyiatzis, G. A.; Lycourghiotis, A.; Kordulis, Ch. *J. Phys. Chem. B* **1998**, *102*, 8459.

(12) Berndt, H.; Martin, A.; Brückner, A.; Schreier, E.; Müller, D.; Kosslick, H.; Wolf, G.-U.; Lücke, B. *J. Catal.* **2000**, *191*, 384.

(13) Chatterjee, M.; Iwasaki, T.; Hayashi, H.; Onodera, Y.; Ebina, T.; Nagase, T. *Chem. Mater.* **1999**, *11*, 1368.

(14) Xiong, G.; Li, C.; Li, H.; Xin Q.; Feng, Z. *Chem. Commun.* **2000**, 677.

(15) Luan, Z.; Xu, J.; He, H.; Klinowski, J.; Kevan, L. *J. Phys. Chem.* **1996**, *100*, 19595.

(16) Wei, D.; Wang, H.; Feng, X.; Chueh, W.-T.; Ravikovitch, P.; Lyubovsky, M.; Li, C.; Takeguchi, T.; Haller, G. L. *J. Phys. Chem. B* **1999**, *103*, 2113.

(17) Mathieu, M.; Van Der Voort, P.; Weckhuysen, B. M.; Rao, R. R.; Catana, G.; Schoonheydt, R. A.; Vansant, E. F. *J. Phys. Chem. B* **2001**, *105*, 3393.

(18) Van Der Voort, P.; Baltes, M.; Vansant, E. F. *J. Phys. Chem. B* **1999**, *103*, 10102.

(19) Van Der Voort, P.; Morey, M.; Stucky, G. D.; Mathieu, M.; Vansant, E. F. *J. Phys. Chem. B* **1998**, *102*, 585.

(20) Morey, M.; Davidson, A.; Eckert, H.; Stucky, G. *Chem. Mater.* **1996**, *8*, 486.

(21) Luan, Z.; Bae, J. Y.; Kevan, L. *Chem. Mater.* **2000**, *12*, 3202.

metal oxides have rarely been explored as a support material. Considering that the effect of support materials is an issue that has been widely disputed in the chemistry of catalysis, it is important to investigate the properties of the supports used for the transition metal mesoporous oxides. It is accepted in general that the reactivity of V catalysts depend not only on V loading but also on the nature of the oxide support, which strongly influences the structure and dispersion of the vanadium species.^{22–24} The specific catalytic properties of supported vanadia catalysts have usually been attributed to the coordination environment of the V species. However, it is more difficult to synthesize mesoporous transition metal oxides with mesostructural ordering and a high surface area than it is to prepare mesoporous silicas.^{25,26}

Antonelli²⁷ has succeeded in preparing phosphorus-free mesoporous titania using a dodecylamine template. Yoshitake et al.²⁸ have optimized the synthetic conditions to obtain mesoporous titania with a BET surface area exceeding $1200 \text{ m}^2 \cdot \text{g}^{-1}$ and with uniform pore channels that vary from 2.3 to 3.4 nm. The bulk phase of titania is inevitably amorphous,²⁸ unlike mesoporous anatase prepared with triblock copolymer templates.²⁹ In addition, approximately 37% of the titanium atoms are 5-fold coordinated.³⁰ These two features have never been found in the catalytic materials in bulk titanium oxides. These are either crystalline rutile or anatase, which are composed of 6-fold coordinated Ti. Considering that the activity and selectivity of catalytic oxidation reactions on vanadia are generally sensitive to the valence and coordination of the V ions, and that vanadia on anatase or rutile exhibits unique catalyses,^{3–5,7,8,10,11,22–24} then mesoporous titania possibly has unsurpassed properties as a support material for vanadium catalysts.

In this paper, we present the preparation procedure, the mesostructure, and the valence and coordination structure of vanadium incorporated into mesoporous titania, as well as reporting the catalytic performance in propene oxidation. The catalysts were prepared either by direct incorporation or by postsynthesis impregnation. The results are compared with those of vanadium oxide supported on conventional nonporous titania.

Experimental Section

Chemicals. Reagent-grade dodecylamine ($\text{C}_{12}\text{H}_{25}\text{NH}_2$) was purchased from Tokyo Kasei Kogyo Co., Ltd. Titanium tetraisopropoxide $\text{Ti}(\text{O}^i\text{Pr})_4$ (Chameleon Reagent, >99%), vanadium oxytriisopropoxide $\text{VO}(\text{O}^i\text{Pr})_3$ (Aldrich, >98%), and *p*-toluenesulfonic acid (Tokyo Kasei Kogyo Co., Ltd., >99%) were also purchased commercially. These reagents were used as received without further purification. Conventional titania support, JRC-TIO-4, is distributed by the Catalysis Society of Japan.

The composition is $\text{TiO}_2 > 99.5\%$, $\text{Al}_2\text{O}_3 < 0.3\%$, $\text{SiO}_2 < 0.2\%$, $\text{Fe}_2\text{O}_3 < 0.01\%$, $\text{Cl} < 0.3\%$, and heavy metals $< 5 \text{ ppm}$. The average particle size is ca. 21 nm, the specific surface area is $50 \pm 15 \text{ m}^2 \cdot \text{g}^{-1}$, and the isoelectric point is $\text{pH} = 6.6$. The bulk phase is mainly anatase. Propene (>99%) and oxygen (>99.95%) were purchased from Takachiho Pure Gas Co.

Synthesis of V-Meso TiO_2 by Direct Incorporation. A typical procedure is as follows. Water (40 g) was added slowly to a mixture of titanium tetraisopropoxide (8.0 g), vanadium oxytriisopropoxide (0.068–1.4 g), and dodecylamine (2.6 g) at 273 K. After the addition of 0.1 M HCl (1.6 cm^3), the mixture was allowed to stand overnight and then transferred to a Teflon container in an oven at 333 K. After 4 d, the solution was filtered and washed with methanol and diethyl ether. The white solid was collected and dried in an oven at 373 K for 1 d before being transferred into a Pyrex test tube, which was evacuated at 453 K by a vacuum pump. After evacuation for 2 h, the tube was sealed. The co-condensation of the alkoxides of titanium and vanadium was completed by heating the powder in the tube at 453 K for 10 d. The resulting solid is denoted as “thermally treated.” This solid was treated with *p*-toluenesulfonic acid to extract the template. The powder was then dried at 373 K for 2 h and calcined at 523 K for 2 h. No nitrogen (<0.01%) was detected by the elemental analysis after template extraction. Ti/V in the gel was 100, 50, 30, 10, and 5. The ratio in thermally treated and extracted V-mesoporous TiO_2 (denoted as V-meso TiO_2) was determined by ICP analysis.

Pure mesoporous titania was obtained if no vanadium oxytriisopropoxide was added into the starting mixture.

Preparation of V/Meso TiO_2 and V/JRC-TIO-4 Impregnation Catalysts. Pure mesoporous titania prepared by the method described above was impregnated with a 2-propanol solution of vanadium oxytriisopropoxide. After standing overnight, the mixture was dried and calcined at 523 K for 2 h. In addition to this V/mesoporous TiO_2 catalyst (denoted as V/meso TiO_2), a conventional nonporous impregnation catalyst was prepared with a JRC-TIO-4 support by the same procedure.

Characterization. The X-ray diffraction (XRD) patterns of the catalysts were recorded using an XL Labo diffractometer (MAC Science Co., Ltd.) with $\text{Cu K}\alpha$ radiation. Nitrogen adsorption–desorption isotherms were measured with a BELSORP 28SA (BEL Japan Inc.) after the sample was heated to 473 K in vacuo.

X-ray absorption experiments were carried out in the beamline BL-9A of Photon Factory, High Energy Accelerator Research Organization, Tsukuba, Japan (Proposal 2002G269), with a ring energy of 2.5 GeV and a stored current of 300–450 mA. A Si(111) double-crystal monochromator was used. The incident X-rays were focused and the higher harmonics were removed by total reflection on a Rh–Ni composite mirror. A conventional transmission mode was employed with detection by gas ion chambers. The V K edge spectra were overlaid on a large absorption due to the support titanium.^{31–33} When the thickness of 1 wt % V-meso TiO_2 was determined under conditions where the maximum absorbance was less than 3, the edge jump obtained did not exceed 0.046. Although a qualitative determination of the structural parameters by EXAFS is difficult to achieve because of the background absorption of TiO_2 , we obtained XANES spectra of sufficient quality to distinguish that oxidation and the coordination states of vanadium for the oscillation of Ti K edge EXAFS is negligible at the edge of V. Despite the small edge jumps, the measurement of each spectrum was completed within 30 min.

For ESR measurements, samples were loaded into 3 mm o.d. \times 2 mm i.d. quartz tubes. The spectra were recorded at

(22) Gao, X.; Wachs, I. E. *J. Phys. Chem. B* **2000**, *104*, 1261.

(23) Olthof, B.; Khodakov, A.; Bell, A. T.; Iglesia, E. *J. Phys. Chem. B* **2000**, *104*, 1516.

(24) Topsøe, N.-Y.; Dumesic, J. A.; Topsøe, H. *J. Catal.* **1995**, *151*, 241.

(25) Sayari, A.; Liu, P. *Microporous Mesoporous Mater.* **1997**, *12*, 149.

(26) Schüth, F. *Chem. Mater.* **2001**, *13*, 3184.

(27) Antonelli, D. *Microporous Mesoporous Mater.* **1999**, *30*, 315.

(28) Yoshitake, H.; Sugihara, T.; Tatsumi, T. *Chem. Mater.* **2002**, *14*, 1023.

(29) Yang, P.; Zhao, D.; Margolese, D. I.; Chmelka, B. F.; Stucky, G. D. *Nature* **1998**, *396*, 152.

(30) Yoshitake, H.; Sugihara, T.; Tatsumi, T. *Stud. Surf. Sci. Catal.* **2002**, *141*, 251.

(31) Kozłowski, R.; Pettifer, R. F.; Thomas, J. M. *J. Phys. Chem.* **1983**, *87*, 5176.

(32) Izumi, Y.; Kiyotaki, F.; Yoshitake, H.; Aika, K.; Sugihara, T.; Tatsumi, Y.; Tanizawa, Y.; Shido, T.; Iwasawa, Y. *Chem. Commun.* **2002**, 1154.

(33) Izumi, Y.; Kiyotaki, F.; Yoshitake, H.; Aika, K.; Sugihara, T.; Tatsumi, Y.; Tanizawa, Y.; Shido, T.; Iwasawa, Y. *Chem. Lett.* **2002**, 1154.

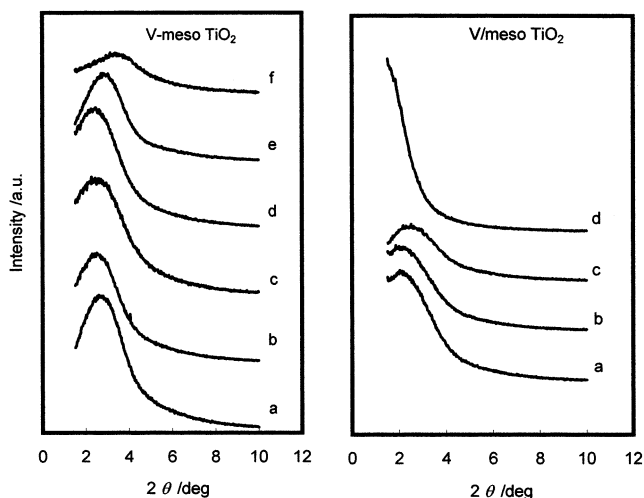


Figure 1. X-ray diffraction patterns of template extracted V-meso TiO₂ (by direct incorporation) and calcined V/meso TiO₂ (by impregnation). The Ti/V of V-meso TiO₂ is ∞ (a), 71 (b), 66 (c), 45 (d), 20 (e) and 12 (f). That of V/meso TiO₂ is 100 (a), 50 (b), 30 (c) and 10 (d).

room temperature on a JES-ME-3X resonance spectrometer (JEOL) calibrated with a DPPH standard ($g = 2.0036$).

Catalytic Oxidation of Propene. The oxidation of propene was carried out in a closed circulating reactor made from Pyrex with a dead volume of 150 cm³. After being inserted into the reactor, the catalyst was calcined at 523 K for 2 h and evacuated at the same temperature for 1 h. The reaction started when the gas mixture of oxygen and propene was introduced to the catalyst at 473 K. The products were analyzed by gas chromatography.

Results and Discussion

Mesostructure of V-Meso TiO₂ and V/Meso TiO₂.

The X-ray diffraction patterns of template-extracted V-meso TiO₂ and V/meso TiO₂ are shown in Figure 1. Only a single peak was observed between $2\theta = 2-4^\circ$ in V incorporated catalysts, just like pure mesoporous titania (Figure 1 a). Because of the lack of reflections from higher indices, we have attributed the structure of mesoporous titania as being wormhole-like, which was supported by TEM photographs.²⁸ Because the peaks were not significantly broadened at Ti/V = ∞–20, the mesostructure of V-meso TiO₂ is assigned to a wormhole-motif. The peak shifted slightly to lower angles in Ti/V = 71, 66, and 45. The reverse shift was observed at Ti/V = 20 and 12. On the other hand, the width of the peak is significantly larger in the impregnation catalysts, V/meso TiO₂, suggesting that the impregnation process causes disordering of the mesostructure. The peak shifted according to the V loading and disappeared completely at Ti/V = 10. Figure 2 shows a few examples of nitrogen adsorption–desorption isotherms and BJH pore size distributions of V-meso TiO₂. No significant differences in the type of the isotherms were found between these plots and those of pure mesoporous titania,²⁸ which has relatively small and uniform mesopores. The pore sizes of V-meso TiO₂ are uniform and almost the same at 2.5–2.6 nm.

Mesostructural parameters calculated from the plots in Figures 1 and 2 are summarized in Table 1. The results of the elemental analysis are also shown in the table. The Ti/V ratio decreases for each step in the

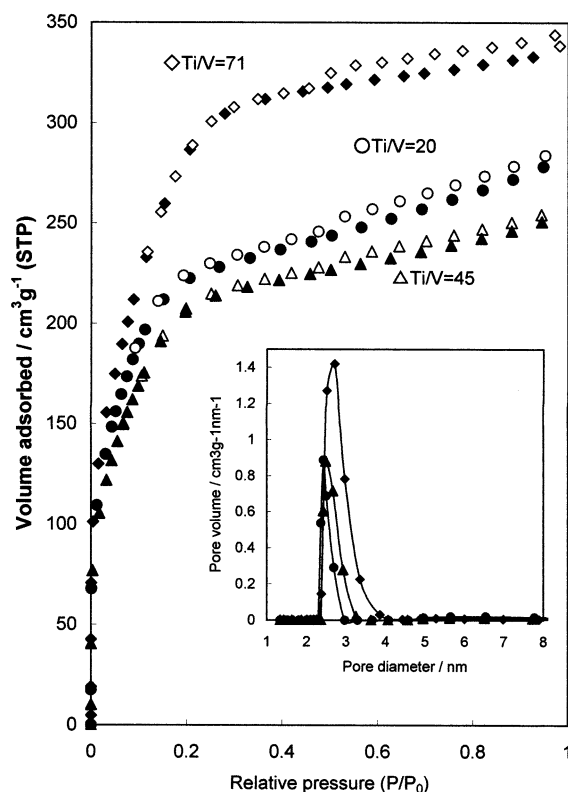


Figure 2. Nitrogen adsorption/desorption isotherms and BJH pore size distributions of V-meso TiO₂. Pore size distributions are derived from the adsorption branch.

Table 1. Structural Parameters of Mesoporous Titania, V-Mesoporous Titania Catalyst Prepared by Direct Incorporation, and V/Mesoporous Titania Catalyst Prepared by Impregnation

gel	Ti/V		d^a (nm)	S_{BET}^b (m ² ·g ⁻¹)	$2R_p^c$ (nm)	V_p^d (cm ³ ·g ⁻¹)
	thermally treated	extracted				
	mesoporous TiO ₂					
			3.27	1139	2.7	0.527
	V-meso TiO ₂					
100	66	71 (0.89)	3.59	1030	2.6	0.493
50	59	66 (0.96)	3.65	675	2.6	0.347
30	33	45 (1.4)	3.65	731	2.5	0.351
10	11	20 (3.1)	3.18	788	2.5	0.356
5	6	12 (5.0)	2.61	228	4.8	0.114
	V/meso TiO ₂					
	100 (0.63)		4.20	1075	2.7	0.524
	50 (1.3)		4.16	722	2.7	0.353
	30 (2.1)		3.62	593	2.7	0.280
	10 (6.0)		^e	350	3.7	0.213

^a Correlated distance of the channel. ^b BET specific surface area. ^c Most probable pore diameter. ^d Pore volume. ^e Not determined because of the broadness of the diffraction. The numbers in the parentheses are the V loading shown as wt %.

preparation of V-meso TiO₂. The concentration of vanadium is possibly caused by the stability of the vanadium oxyhydroxide in basic and acidic media. The correlated distance of the pores, $d = \lambda/2\sin \theta$, changes according to the position of the peak maximum of the X-ray diffraction. The distance d is larger in V-meso TiO₂ than in mesoporous titania between Ti/V = ∞ and 45, whereas it is significantly smaller below Ti/V = 20. Although the origin of this change in d is not clear, $d - 2R_p$, which is a measure of the mesopore wall thickness, is more than that for pure titania except when Ti/V =

12, suggesting that the walls are thickened by the incorporation of vanadium. The thickness $d - 2R_p < 0$ at $\text{Ti}/\text{V} = 12$ implies a destruction of the pore structure, which agrees with the surface area noticeably lower ($228 \text{ m}^2 \cdot \text{g}^{-1}$) than that of the other V-meso TiO_2 ($675\text{--}1030 \text{ m}^2 \cdot \text{g}^{-1}$). We conclude that the direct incorporation method can prepare V-meso TiO_2 catalyst with $\text{Ti}/\text{V} = 20$ (i.e., loading at 3.1 wt % as V metal) where the original mesostructure of the mesoporous titania remains. As shown in Figure 2, the distributions of the pore size are narrow, which is advantageous for molecular sieving in catalytic reactions. The d of the V/meso TiO_2 is significantly larger than that of pure mesoporous titania, whereas the surface area decreases according to the V loading. The pore diameter is not different from that in the pure mesoporous titania, except for the sample with $\text{Ti}/\text{V} = 10$. Despite a considerable degradation in mesostructural order of the channels, the pore diameter remains the same in the impregnation catalyst.

In V-MCM-41¹³ and V-MCM-48¹⁷ prepared by a direct-incorporation method, a broadening of the XRD patterns occurred, the pore size distributions were as narrow as the original framework, and the surface area was increased. Although the authors of these studies did not discuss the increase in the surface area by incorporating vanadium, this phenomenon makes a good contrast to V-meso TiO_2 . On the other hand, postsynthesis impregnations on MCM-41,¹² MCM-48,²⁰ and SBA-15,²¹ and grafting on MCM-48¹⁹ without the use of solvent resulted in a decrease in the surface area. In addition to a narrow distribution of pore sizes, XRD broadening occurred just as it did in direct incorporation, though reflections from higher indices clearly appeared in V/MCM-48.^{19,20} The degree of degradation of the XRD patterns in V/meso TiO_2 is undoubtedly larger than that for V/MCM-48. This difference is attributed to the weakness of the framework structure of mesoporous titania. MCM-48 is usually obtained by calcination at around 773 K,^{19,20} while a significant decrease of the surface area was observed when mesoporous titania was treated with air at 673 K.³⁰

Local Structure of Vanadium. XANES spectra of V-meso TiO_2 and V/meso TiO_2 are compared with that of V/JRC-TIO-4 in Figure 3. The pre-edge peak is attributed to the $1s \rightarrow 3d$ transition, which is dipole forbidden in the octahedral VO_6 units that have a center of inversion.³⁴ The lowering of the symmetry, which is accompanied with the combination of $3d$ - $4p$ mixing and overlap of the metal $3d$ orbitals with the $2p$ of oxygen, allows a pre-edge absorption. It is also well-known that the position and the intensity of the peak are sensitive to the valence and coordination of the metal.^{34,35} The pre-edge peaks of V/meso TiO_2 and V/JRC-TIO-4 appeared at the same position as that of V_2O_5 . This is 5.6 eV higher than the edge position of V metal. On the other hand, the pre-edge absorption of V-meso TiO_2 occurred at 4.6 eV vs the edge position of V metal, which is almost the same as the pre-edge position of V_2O_4 (at 4.5 eV).^{33,34} In addition to the pre-edge, we found

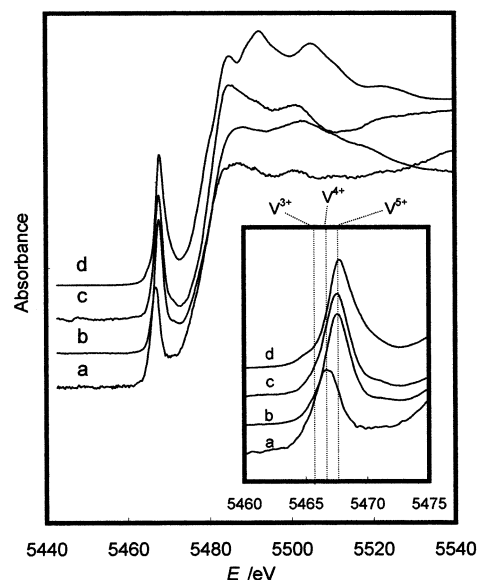


Figure 3. V K Edge XANES spectra of V-meso TiO_2 ($\text{Ti}/\text{V} = 12$) (a) and V-meso TiO_2 ($\text{Ti}/\text{V} = 100$) (b), in comparison with those of V/JRC-TIO-4 (1.2%) (c) and V_2O_5 (d). The inset is the expanded pre-edge absorptions.

similarities in the characteristic absorption positions between V-meso TiO_2 and V_2O_4 : the pre-edge threshold (3.6 vs 3.5 eV, respectively), the main edge (13.8 vs 14 eV, respectively), and the $1s \rightarrow 4p$ transition (25.9 vs 26.2 eV, respectively).³⁴ The relative intensity of the absorbance was almost the same as that for V_2O_4 . These spectral similarities indicate that V in V-meso TiO_2 has a +4 valence and its coordination symmetry is a distorted octahedron or square pyramid. The fwhm (= 2.5 eV), which is not broadened from those of V_2O_5 or V_2O_4 , suggests the uniformity of the structure.

In addition to the agreement of the position of the pre-edge absorptions in V/meso TiO_2 , V/JRC-TIO-4, and V_2O_5 , the relative peak intensities (= peak height divided by the edge jump) of these catalysts and oxide are almost the same: 0.78, 0.73, and 0.77 for V/meso TiO_2 , V/JRC-TIO-4, and V_2O_5 , respectively. These positions and intensities permit assignment of most of the V species in V/meso TiO_2 and V/JRC-TIO-4 to being in a pentavalent state in distorted square pyramidal coordinations. The post-edge absorptions of V/meso TiO_2 , V/JRC-TIO-4, and V_2O_5 are not similar. The position of the absorption usually attributed to the $1s \rightarrow 4p$ transitions³⁴ is rather similar between V/meso TiO_2 (26.1 eV vs the edge position of V metal) and NH_4VO_3 (26.6 eV), and between V/JRC-TIO-4 (24.1 eV) and CrVO_4 (24.2 eV). NH_4VO_3 and CrVO_4 are composed of distorted tetrahedral coordinations despite the pre-edge absorption showing lower intensity than V in V_2O_5 (distorted square pyramid). This disagreement suggests a local environment of V in these supported catalysts different from that in V_2O_5 , probably because of the lack of linkage of the VO_n units. A similar post-edge absorption has been reported in vanadium in a monomeric dispersion with polyvanadate domains on an alumina support.²³ We obtained the same XANES feature in 1.2 and 3.2 wt % V/JRC-TIO-4, though 10 wt % V/JRC-TIO-4 showed the same spectrum as V_2O_5 .

Previous XANES studies have claimed that vanadium in supported vanadia catalysts is 5+ valent under

(34) Wong, J.; Lytle, F. W.; Messmer, R. P.; Maylotte, D. H. *Phys. Rev. B* **1984**, *30*, 5596.

(35) Nabavi, M.; Taulelle, F.; Sanchez, C.; Verdaguier, M. *J. Phys. Chem. Solids* **1990**, *51*, 1375.

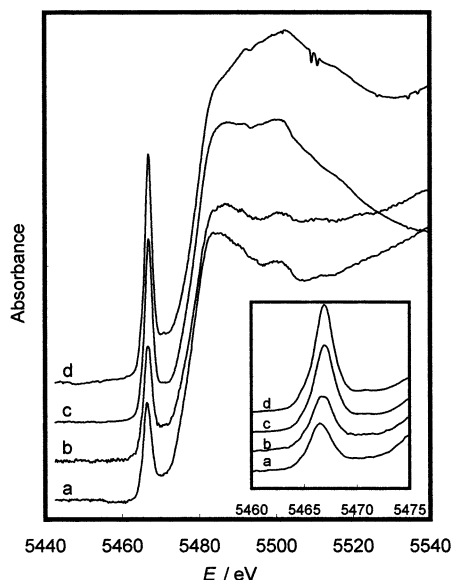


Figure 4. V K Edge XANES spectra of V-meso TiO₂ (Ti/V = 12) after template extraction (a) with V-meso TiO₂ (Ti/V = 71) after template extraction (b), after thermal treatment at 453 K (c), and after hydrothermal synthesis at 333 K (d). The pre-edge region was expanded in the inset.

atmospheric conditions (air-exposed).^{16,23,36–40} It has been reported that the pre-edge position of V in a V/anatase catalyst is exactly the same as V₂O₅, just as for the present result for V/JRC-TIO-4.⁴¹ On the other hand, V⁴⁺ has been observed in VPO/SiO₂⁴² and VAPO-5⁴³ catalysts under reduced or dehydrated conditions. The vanadium oxide dispersed on titania support accelerates the phase transformation from anatase into rutile, and, during this phase transition, a part of vanadia is reduced and incorporated into the rutile structure.^{44,45} However, the transition temperature of this phase transformation is above 800 K, which is much higher than the oxidation temperature of V-meso TiO₂ (523 K). Considering these previous studies, a V⁴⁺ species formed uniformly under atmospheric conditions is a unique property of the V-meso TiO₂ catalyst. This reveals that the V⁴⁺ is stabilized extraordinarily in the framework structure of V-meso TiO₂.

Figure 4 shows the edge spectra of V-meso TiO₂ with a different V loading and in different stages of preparation. The intensity and position of the pre-edge absorption of V-meso TiO₂ loading at Ti/V = 71 are the same as those at Ti/V = 12, and no significant difference was

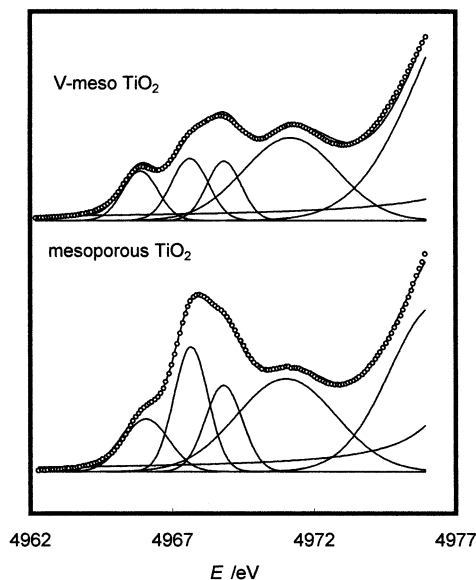


Figure 5. Pre-edge absorption in Ti K edge XANES spectra of mesoporous TiO₂ and V-meso TiO₂.

found in the post-edge region. The spectra observed in Ti/V = 12 and 71 were the same as those obtained for all the other loadings shown in Table 1 (Ti/V = 20, 45, and 66). This can be seen as evidence of the independence of the local structure of V from the loading and the uniformity of the structure on the condition that the mesostructure is formed. By contrast, we observe a difference among the samples after hydrothermal synthesis at 333 K, after heat treatment at 453 K, and after template extraction (Figure 4). The relative intensity of the pre-edge is 1.2 and 0.94 for V after hydrothermal synthesis at 333 K and after heat treatment at 453 K, respectively, whereas it is 0.59 for extracted V-meso TiO₂. On the other hand, the peak position does not shift, suggesting that vanadium is tetravalent at all stages. Because V in the source compound, VO(OⁱPr)₃ is pentavalent, and the transformation into V⁴⁺ undoubtedly occurs during hydrothermal synthesis at 333 K. This stage is a cohydration of the alkoxides of titanium and vanadium and an insertion of the VO_x unit into the latticework of the TiO₂. The strong peak intensity in Figure 4d implies that the symmetry of V is much lowered. Because a significant amount of water is generated during the thermal treatment at 453 K, Ti–OH bonds are converted into Ti–O–Ti bonds at this stage.²⁸ The decrease of the pre-edge absorption implies that V becomes more symmetric in the framework of the mesoporous titania than in the titania gel, which has more Ti–OH groups.

To specify the site of vanadium substitution, we measured the Ti K edge XANES spectra of mesoporous titania and V-meso TiO₂ (Ti/V = 12). The pre-edge peaks are overlaid with the deconvoluting Lorentzian functions in Figure 5. As has been already demonstrated, the pre-edge peaks of Ti in mesoporous TiO₂ are composed of the absorptions due to 5- and 6-fold coordinated Ti.^{30,46} The results of the deconvolution of the pre-edge peaks are summarized in Table 2. The ratio of molar absorption coefficients of these species can be

(36) Anderson, G. *Acta Chem. Scand.* **1956**, *10*, 623.
 (37) Tanaka, T.; Yamashita, H.; Tsuchitani, R.; Funabiki, T.; Yoshida, S. *J. Chem. Soc., Faraday Trans. 1* **1988**, *84*, 2987.
 (38) Takenaka, S.; Tanaka, T.; Yamazaki, T.; Funabiki, T.; Yoshida, S. *J. Phys. Chem. B* **1997**, *101*, 9035.
 (39) Inumaru, K.; Okuhara, T.; Misono, M.; Matsubayashi, N.; Shimada, H.; Nishijima, A. *J. Chem. Soc., Faraday Trans.* **1992**, *88*, 625.
 (40) Rulkens, R.; Male, J. L.; Terry, K. W.; Olthof, B.; Khodakov, A.; Bell, A. T.; Iglesia, E.; Tilley, T. D. *Chem. Mater.* **1999**, *11*, 2966.
 (41) Burkardt, A.; Weisweiler, W.; van den Tillaart, J. A. A.; Schafer-Sindlinger, A.; Lox, E. S. *Top. Catal.* **2001**, *16/17*, 369.
 (42) Birkeland, K. E.; Babitz, S. M.; Bethke, G. K.; Kung, H. H.; Coulson, G. W.; Bare, S. R. *J. Chem. Phys. B* **1997**, *101*, 6895.
 (43) Cheng, H. Y.; Yang, E.; Lai, C. J.; Chao, K. J.; Wei, A. C.; Lee, J. F. *J. Phys. Chem. B* **2000**, *104*, 4195.
 (44) Roozeboom, F.; Mittelmeijer-Hazeleger, M. C.; Moulijin, J. A.; Medema, J.; de Beer, V. H.; Gellings, P. J. *J. Phys. Chem.* **1980**, *84*, 2783.
 (45) Bond, G. C.; Tahir, F. *Appl. Catal.* **1991**, *71*, 1.

(46) Yoshitake, H.; Sugihara, T.; Tatsumi, T. *Phys. Chem. Chem. Phys.* **2003**, *5*, 767.

Table 2. Results of Deconvolution of the Pre-Edge Peaks of the XANES Spectra

	$I(4967.6 \text{ eV})$ arb. unit	$I(4968.8 \text{ eV})$ arb. unit	$^{51}\text{Ti}/(^{51}\text{Ti} + ^{63}\text{Ti})$
mesoporous TiO_2	1.4	0.91	0.37
V-meso TiO_2 (Ti/V = 12)	0.73	0.68	0.29
V/meso TiO_2 (Ti/V = 10)	1.1	0.72	0.36

empirically deduced: $\epsilon(^{51}\text{Ti})/\epsilon(^{63}\text{Ti}) = 8/3$.⁴⁶ A clear decrease in the population of 5-fold titanium is found in V-meso TiO_2 . The reduction by 8% of the total Ti agrees well with the vanadium content, $\text{V}/\text{Ti} = 1/12 = 0.083$, implying that the ^{51}Ti site is substituted by vanadium. The 5-fold Ti site is coordinated by oxygen atoms at the corners of a square pyramid. Because of having the same valence, it is also reasonable to attribute the coordination of vanadium in V-meso TiO_2 to being a square pyramid. This is consistent with the V K edge XANES spectrum.

On the other hand, the population of ^{51}Ti remains in almost the same ratio in V/meso TiO_2 . We did not observe the substitution of a specific site of the mesoporous titania by the impregnation method.

The V K edge XANES spectra of V/meso TiO_2 in different loadings are compared in Figure 6. No meaningful differences are found either in the pre-edge or in the post-edge of these spectra, suggesting that V is uniformly dispersed on mesoporous TiO_2 between $\text{Ti}/\text{V} = 10$ and 100. On the other hand, for V/JRC-TIO-4, the spectra did not change between 1.2 and 3.2 wt % (not shown in the figure). The uniformity of the local structure of V is suggested for V/JRC-TIO-4 below 3.2 wt %.

The ESR spectra of V-meso TiO_2 and V/meso TiO_2 were measured under atmospheric conditions (air-exposed) or when they were sealed in a vacuum after evacuation at 473 K. The results are shown in Figure 7. We observe an axially symmetric set of hyperfine splitting (*hfs*) multiples originating from vanadyl VO^{2+} species coupled to the nuclear spin of ^{51}V . This *hfs* is characteristic of well-isolated vanadyl species in square pyramidal or distorted octahedral coordinations.^{12–13,15,21,47} The absence of a broad isotropic line superimposed on the *hfs*, as is often observed in supported vanadium catalysts, indicates that there are no significant amounts of vanadyl species interacting with each other.^{12,15} The spin Hamiltonian parameters calculated from Figure 4 are summarized in Table 3. Little difference is found among all of the parameters of hydrated and dehydrated V-meso TiO_2 , including B , a measure for the tetragonal distortion of the vanadium coordination sphere.⁴⁸ On the other hand, for V/meso TiO_2 , g_{\parallel} and g_{\perp} were changed by evacuation just as is often observed in supported V catalysts,^{12–13,15,21,47–50} and B increased from 2.6 to 6.9. One explanation for the increase of B is that desorption of water molecules induces a shortening of the $\text{V}=\text{O}$ bond and a lengthening of the $\text{V}-\text{O}$ bond in the basal plane of a distorted square pyramid.⁴⁸ The distortion of a vanadyl species by desorption of water is often observed in V supported on silica catalysts.¹²

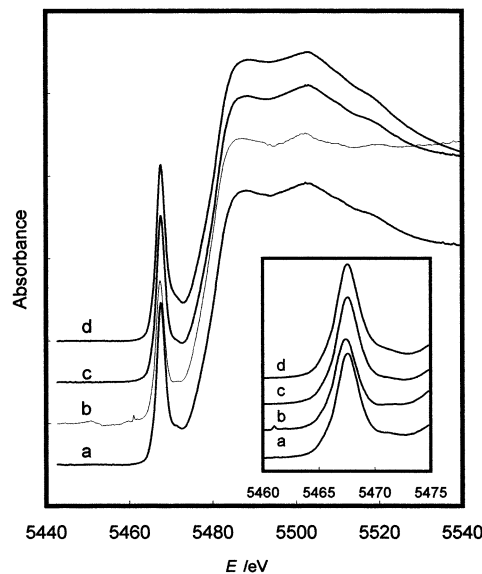


Figure 6. V K Edge XANES spectra of V/meso TiO_2 with $\text{Ti}/\text{V} = 10$ (a), 30 (b), 50 (c), and 100 (d). The pre-edge region was expanded in the inset.

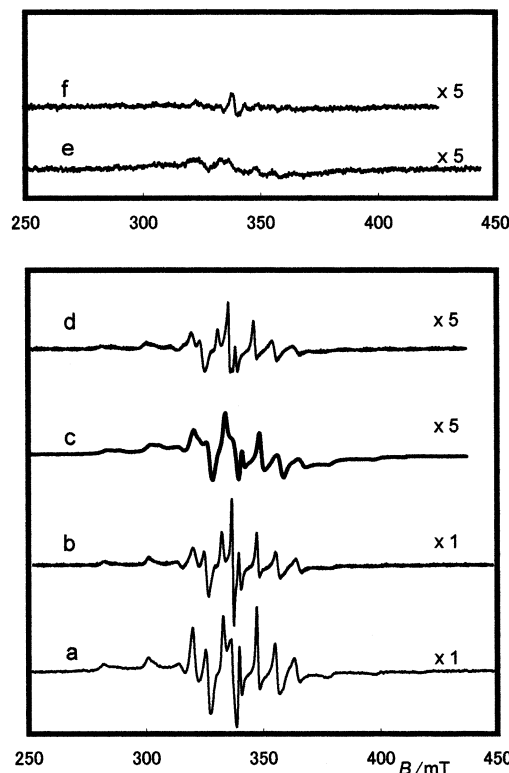


Figure 7. ESR spectra of V-meso TiO_2 ($\text{Ti}/\text{V} = 45$) hydrated under atmospheric condition (a) and evacuated at 473 K (b), and those of V/meso TiO_2 ($\text{Ti}/\text{V} = 50$) hydrated under atmospheric condition (c) and evacuated at 473 K (d), in comparison with those of 1.2 wt % V/JRC-TIO-4 (e) and V- TiO_2 ($\text{Ti}/\text{V} = 100$) prepared without template (f) hydrated in atmosphere.

It has been reported that the ESR signals lack well-resolved *hfs* in vanadium supported on conventional nonporous titanias when it is exposed to atmosphere and measured at room temperature,⁴⁹ contrary to observation for Al_2O_3 .⁵⁰ The results are reproduced in our sample V/JRC-TIO-4 (Figure 7 d).

(47) Gontier, S.; Tuel, A. *Microporous Mater.* **1995**, *5*, 161.

(48) Sharma, V. K.; Wokaun, A.; Baiker, A. *J. Phys. Chem.* **1986**, *90*, 2715.

(49) Inomata, M.; Mori, K.; Miyamoto, A.; Ui, T.; Murakami, Y. *J. Phys. Chem.* **1983**, *87*, 754.

Table 3. ESR Parameters for 1.4% V-Mesoporous TiO₂ and 1.3% V/Mesoporous TiO₂ Catalysts

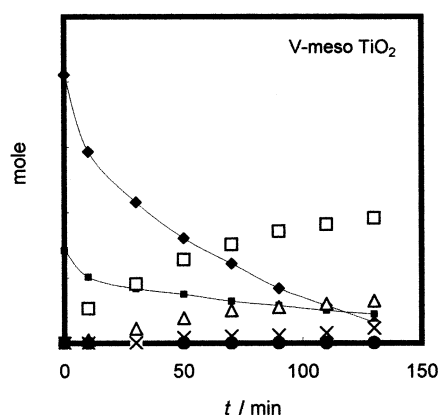
	g_{\parallel}	g_{\perp}	$A_{\parallel}/\text{cm}^{-1}$	A_{\perp}/cm^{-1}	B^a
V-meso TiO ₂ (Ti/V = 45) air-exposed	1.928	1.985	-0.0174	-0.0068	4.3
V-meso TiO ₂ (Ti/V = 45) evacuated	1.925	1.985	-0.0174	-0.0071	4.5
V/meso TiO ₂ (Ti/V = 50) air-exposed	1.925	1.972	-0.0171	-0.0068	2.6
V/meso TiO ₂ (Ti/V = 50) evacuated	1.938	1.993	-0.0172	-0.0073	6.9

$$^a B = (g_{\parallel} - g_e)/(g_{\perp} - g_e).$$

Table 4. Rate of Formation in Propene Oxidation on V/JRC-TIO-4, V-Mesoporous TiO₂ and V/Mesoporous TiO₂ Catalysts^a

	r/min^{-1}					
	O ₂	C ₃ H ₆	CO	CO ₂	H ₂ O	C ₂ H ₅ OH
1.2% V/JRC-TIO-4	-0.043	-0.014	0.012	0.012	0.0026	1.5×10^{-4}
1.4% V-meso TiO ₂	-0.116	-0.030	0.020	0.060	0.0053	1.6×10^{-4}
1.3% V/meso TiO ₂	-0.747	-0.206	0.091	0.279	0.039	5.1×10^{-4}

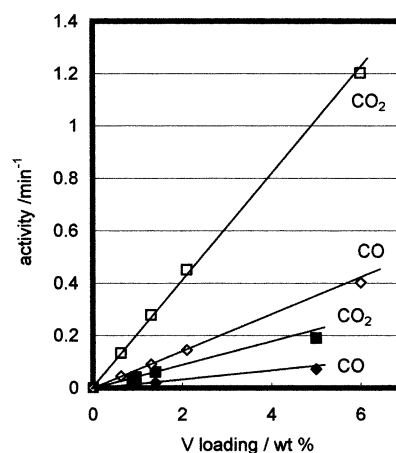
^a r is the molar amount of product per unit mol of V in the catalyst per minute. Reaction temperature was 500 K. Initial pressure of the reactants was $P_{\text{O}_2} = 6.6$ kPa and $P_{\text{C}_3\text{H}_6} = 2.4$ kPa. Note that because the catalytic tests were carried out in a closed reactor, the mass balance does not hold: $-r(\text{C}_3\text{H}_6) \neq [r(\text{CO}) + r(\text{CO}_2)]/3$ and the oxygen consumption rate does not equal to the oxygen appearance in the products.

**Figure 8.** Reaction profile of propene oxidation on V-meso TiO₂ (Ti/V = 45). The symbols are \blacklozenge , O₂; \blacksquare , C₃H₆; \triangle , CO; \square , CO₂; \times , H₂O; and \bullet , C₂H₅OH.

Tetravalent vanadium is the major species in V-meso TiO₂. This means that the ESR spectra describe the behavior of the most abundant V species, unlike other supported V catalysts in the literature. The undisturbed B after evacuation at 473 K implies that this V⁴⁺ species is extremely stable. The origin of abnormal stability can be attributed to the trapping of V into the 5-fold Ti site in the framework of titania. By contrast, the large change in B induced by evacuation indicates that the structure of V⁴⁺ is more sensitive to the adsorbates than V-meso TiO₂. Nevertheless, mesoporous titania is a support that easily generates tetravalent vanadium on itself, showing an ESR signal with hfs at room temperature like V/silica or V/alumina.^{12-13,15,21,47,50}

It should be noted that no signal was found in the ESR of V-TiO₂ prepared without surfactant template. The lack of the resonance indicates that most of the V in this oxide is V⁵⁺ (d^0) and consequently the stabilization of V⁴⁺ is only possible in the wall of the mesopores of titania.

Catalytic Performance. The composition of the gas phase during propene oxidation on V-meso TiO₂ is plotted in Figure 8. CO and CO₂ are the main products, while the production of ethanol is negligible. The partial pressures of oxygen and propene decreased monotonically,

**Figure 9.** Catalytic activity for CO₂ and CO formations on V-meso TiO₂ (\blacksquare , \blacklozenge) and V/meso TiO₂ (\square , \diamond) catalysts with various loading. The activity is expressed by the formation (in mol) per 1 min divided by the amount of V atom (in mol) in the catalyst.

ally, while carbon dioxide and monoxide increased without any induction period, indicating that the serial oxidation of propene \rightarrow CO \rightarrow CO₂ is unlikely.

The activities represented by the rate of molar formation per unit mole of V are listed in Table 4. Because they have almost the same loading and the same high dispersion of V (confirmed by XANES), the differences found in Table 4 are attributable to the properties of one V atom on each support. The CO and CO₂ formation rates on V-meso TiO₂ are respectively 1.7 and 5.0 times higher than those on V/JRC-TIO-4. It should be noted that the selectivity to CO₂, $r(\text{CO}_2)/(r(\text{CO}) + r(\text{CO}_2))$, is different between these catalysts: 0.75 and 0.50 for V-meso TiO₂ and V/JRC-TIO-4, respectively. Although the structure of V⁴⁺ in the framework of mesoporous titania is unchanged with respect to water adsorption/desorption, it is considerably more active than V on a conventional support, JRC-TIO-4, which includes little V⁴⁺ under atmospheric condition.

The impregnation catalyst, V/meso TiO₂, is even more active than V-meso TiO₂. The factors of enhancement of CO and CO₂ formation are 7.6 and 23, respectively. In contrast, the selectivity to CO₂ is not different from that on V-meso TiO₂, 0.75. Although the catalytic

(50) Inomata, M.; Mori, K.; Miyamoto, A.; Ui, T.; Murakami, Y. *J. Phys. Chem.* **1983**, *87*, 761.

performance of vanadium in V/meso TiO₂ is outstanding, the active site and oxidation mechanism has not been clarified by the present experiments. The total oxidation rate, which is defined by $r(\text{CO}) + 2r(\text{CO}_2)$, is 0.036, 0.14, and 0.65 for V/JRC-TIO-4, V-meso TiO₂, and V/meso TiO₂, respectively. This measure indicates that the rate of propene oxidation is 3.9 times and 18 times higher on V-meso TiO₂ and V/meso TiO₂, respectively, than on V/JRC-TIO-4.

The activities to CO and CO₂ are linearly increased with loading of V in V-meso TiO₂ and V/meso TiO₂, as shown in Figure 9, indicating that the active species are uniformly distributed on the surface of the mesoporous titania. The result of XANES spectra (Figures 4 and 6), demonstrating that the local structure of V species is independent of the loading, and the linearity in Figure 9 imply a correlation between the absorber of X-ray and the active species of catalytic oxidation. In the case of V-meso TiO₂, the absorber is tetravalent vanadium and this was assigned to distorted square pyramid fixed in the ⁵¹Ti site. It is, consequently, reasonable to assume that this tetravalent vanadium is attributed to the active species for propene oxidation.

Conclusion

Vanadium-loaded mesoporous titania has been successfully prepared by direct incorporation (maximum loading = 5 wt % as V metal) and postsynthesis

impregnation methods. V K edge XANES reveals that vanadium in V-meso TiO₂ (the catalyst by direct incorporation) is tetravalent. By contrast, the valence and coordination structure of vanadium in V/meso TiO₂ (the catalyst prepared by impregnation) can be assigned as being V⁵⁺. ESR active vanadium (V⁴⁺) is found in both catalysts under atmospheric conditions. The spin Hamiltonian parameters indicate that the coordination of vanadium is a distorted square pyramidal or octahedral coordination environment. In V-meso TiO₂, no significant change in these parameters is induced by an evacuation treatment at 473 K, suggesting that the structure of the vanadium species is more stable than conventional oxide-supported vanadium. Ti K edge XANES spectroscopy shows that the population of 5-fold coordinated Ti in V-meso TiO₂ decreased by the number of V incorporated from that in mesoporous TiO₂. The result implies that V is inserted into the ⁵¹Ti site of the framework structure of mesoporous titania and V is in a square pyramidal coordination. V-meso TiO₂ and V/meso TiO₂ show high activities to propene oxidation. The total rate of oxidation per unit V per min is 0.036, 0.14, and 0.65 for V/JRC-TIO-4 (conventional non porous titanium dioxide), V-meso TiO₂, and V/meso TiO₂, respectively. The selectivity to CO₂ is enhanced on V-meso TiO₂ and V/meso TiO₂.

CM021077K